

## The Simulated Indian Monsoon: A GCM Sensitivity Study

M. J. FENNESSY, J. L. KINTER III, B. KIRTMAN, L. MARX, S. NIGAM, E. SCHNEIDER, J. SHUKLA,  
D. STRAUS, A. VERNEKAR, Y. XUE, AND J. ZHOU

*Center for Ocean-Land-Atmosphere Interactions, Department of Meteorology, University of Maryland, College Park, Maryland*

(Manuscript received 25 October 1992, in final form 17 June 1993)

### ABSTRACT

A series of sensitivity experiments are conducted in an attempt to understand and correct deficiencies in the simulation of the seasonal mean Indian monsoon with a global atmospheric general circulation model. The seasonal mean precipitation is less than half that observed. This poor simulation in seasonal integrations is independent of the choice of initial conditions and global sea surface temperature data used. Experiments are performed to test the sensitivity of the Indian monsoon simulation to changes in orography, vegetation, soil wetness, and cloudiness.

The authors find that the deficiency of the model precipitation simulation may be attributed to the use of an enhanced orography in the integrations. Replacement of this orography with a mean orography results in a much more realistic simulation of Indian monsoon circulation and rainfall. Experiments with a linear primitive equation model on the sphere suggest that this striking improvement is due to modulations of the orographically forced waves in the lower troposphere. This improvement in the monsoon simulation is due to the kinematic and dynamical effects of changing the topography, rather than the thermal effects, which were minimal.

The magnitude of the impact on the Indian monsoon of the other sensitivity experiments varied considerably, but was consistently less than the impact of using the mean orography. However, results from the soil moisture sensitivity experiments suggest a possibly important role for soil moisture in simulating tropical precipitation, including that associated with the Indian monsoon.

### 1. Introduction

It has been found that many general circulation models (GCMs) of the atmosphere have serious deficiencies in simulating the Asiatic monsoon circulation and rainfall, especially over India (WMO 1990). The simulated June–July–August (JJA) 1988 time-mean precipitation from a Center for Ocean–Land–Atmosphere Interactions (COLA) GCM control integration performed with observed sea surface temperature (SST) is low over peninsular India (Fig. 1b) compared to that observed (Fig. 1a, discussed further in section 3). This and other deficiencies in the COLA GCM control simulations over the Indian monsoon region motivated this study.

We performed a number of experiments to test the sensitivity of the Indian monsoon circulation in the COLA GCM. The poor Indian monsoon simulated in the control integration (Fig. 1b) is very similar to that in an earlier version of the COLA GCM that was used in a preliminary study of the interannual variability of the monsoon circulations by Fennessy and Shukla (1990). After analyzing 12 three-month boreal summer integrations using initial and boundary conditions from 1987 and 1988 recommended by the Tropical Oceans

and the Global Atmosphere (TOGA) Monsoon Numerical Experimentation Group (MONEG; WMO 1990), Fennessy and Shukla (1990) concluded that the weakest features of their otherwise realistic seasonal mean simulations were the Indian monsoon circulation and rainfall. The deficiencies of the Fennessy and Shukla (1990) Indian monsoon simulations were insensitive to both the initial atmospheric state and the SST field. The experiments presented here include tests of the model's sensitivity to changes in the height of the orography, vegetation, soil wetness, and cloudiness.

The importance of the Asian landmass as an elevated heat source that helps drive the boreal summer monsoon circulations has long been recognized. Reviews of the literature on this topic are given by Hahn and Manabe (1975), Druryan (1981), and Luo and Yanai (1984). However, our understanding of the exact mechanisms involved continues to expand with the results of more recent research (e.g., Krishnamurti and Ramanathan 1982; Luo and Yanai 1984; Barnett et al. 1989). Hahn and Manabe (1975) established the crucial importance of mountains to the south Asian monsoon circulation in numerical simulations done with an 11-level global model with and without mountain topography. Druryan (1982) found that lowering and flattening the Himalayas in simulations with a coarse resolution GCM ( $8^\circ$  by  $10^\circ$  grid, 5 vertical lev-

---

*Corresponding author address:* Dr. M. J. Fennessy, COLA, 4041 Powder Mill Rd., Suite 302, Calverton, MD 20705.

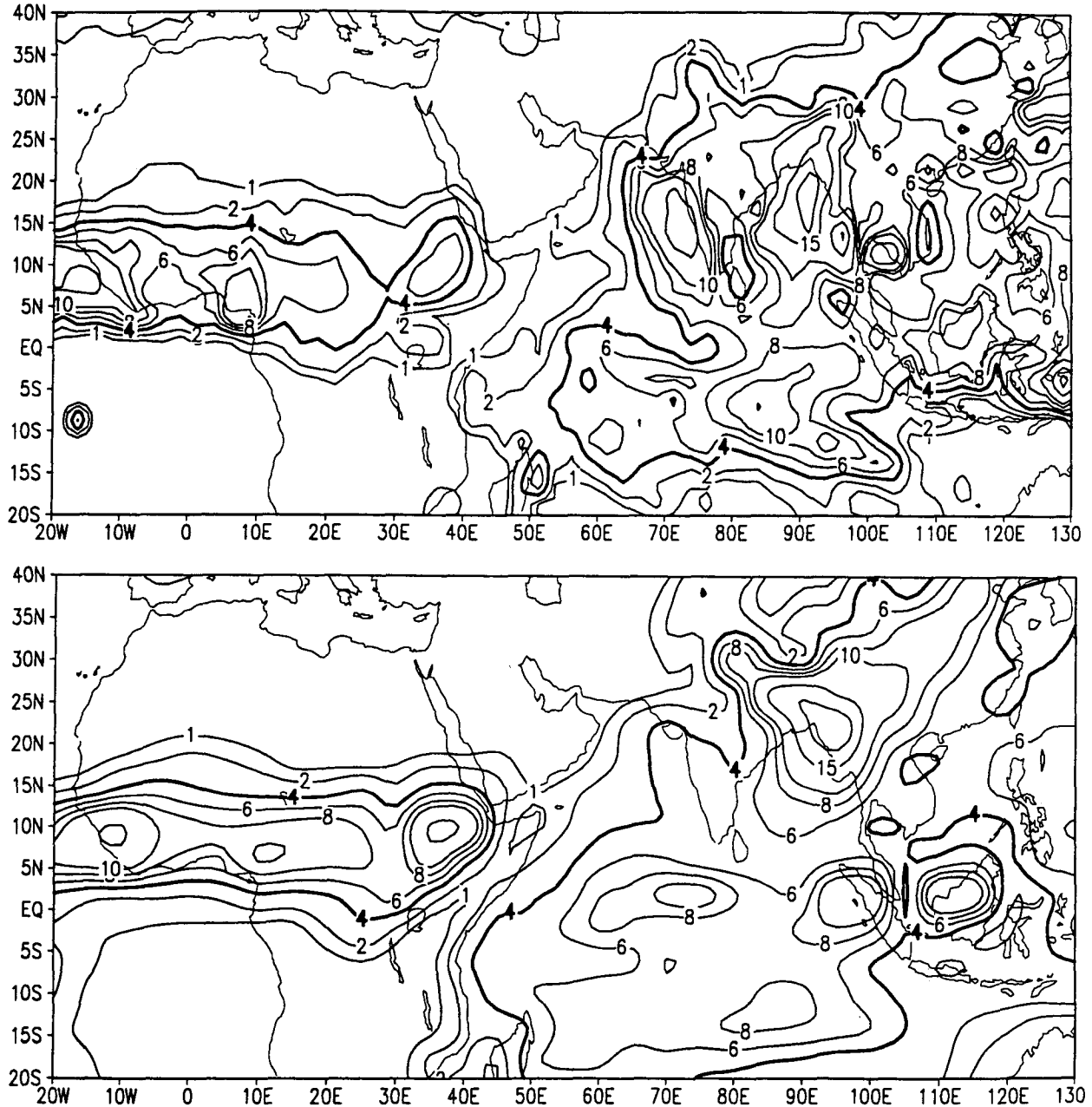


FIG. 1. (a) Observed JJA mean precipitation (see text). (b) Control integration JJA mean precipitation. Contours are 1, 2, 4, 6, 8, 10, 15, 20, and 25,  $\text{mm day}^{-1}$ . JJA mean 850-mb wind for (c) ECMWF analysis and (d) control integration. Contour interval is  $5 \text{ m s}^{-1}$ .

els) resulted in more subtle circulation deteriorations, including a delay in the monsoon onset.

A recent paper by Bhaskar Rao et al. (1991), examined the influence of several land boundary conditions on the Asian summer monsoon. In their simulations with a relatively coarse resolution GCM ( $4^\circ$  by  $5^\circ$  grid, 5 vertical levels), they found that elevating the topography globally both deteriorated the Asian monsoon circulation and increased the Indian monsoon precipitation, a seemingly contradictory result.

We investigate the choice of orography used in the COLA GCM, in this case either a silhouette (enhanced) orography (Mesinger et al. 1988) or a mean orography. The mean orography is computed as an arithmetic mean from the 10-min resolution U.S. Navy modal terrain height data. The silhouette orography is computed from the mean of the highest peaks of the Navy modal terrain height data over each grid area. It is similar to the envelope orography used in several other GCMs (Wallace et al. 1983). Our results show that

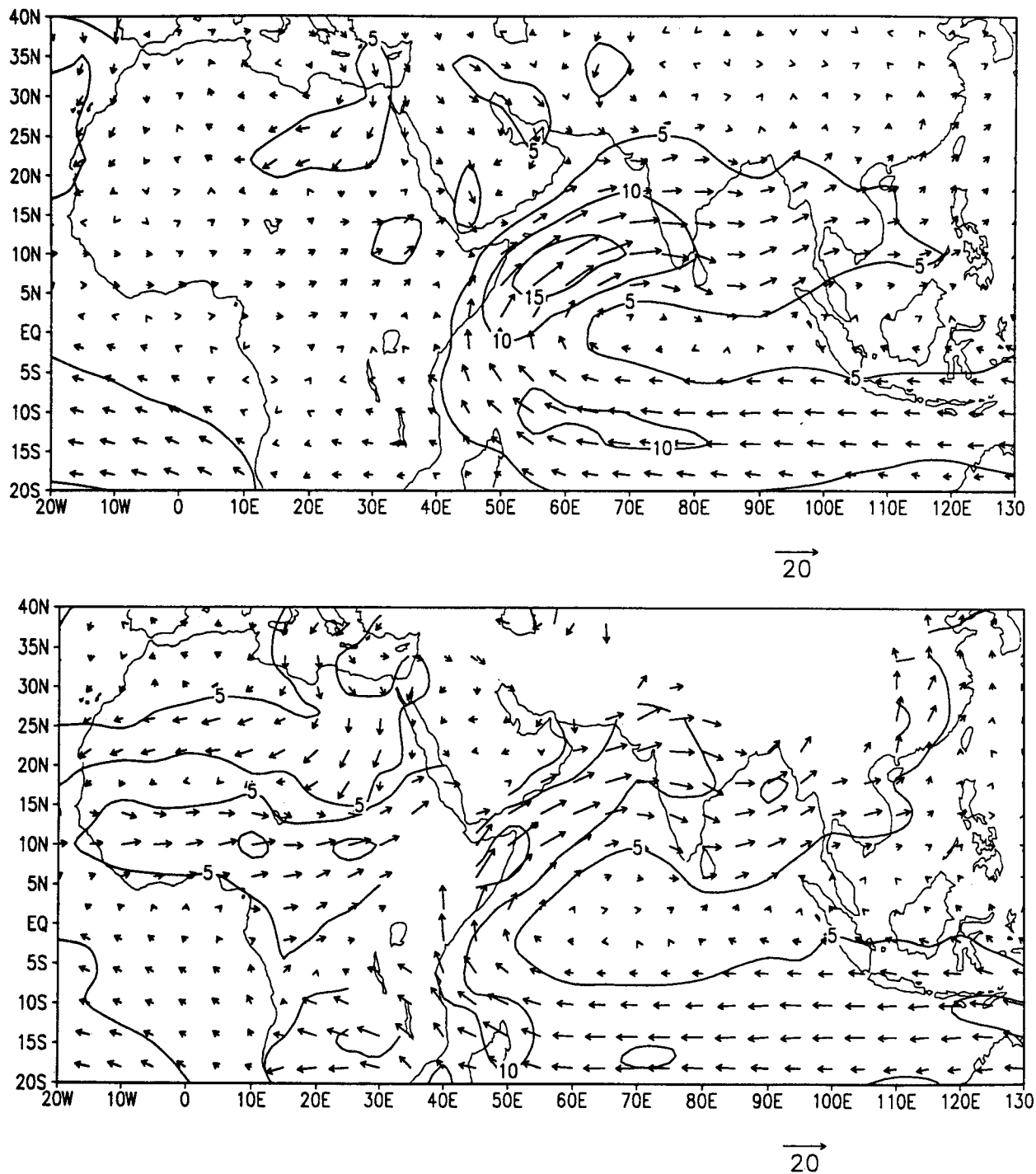


FIG. 1 (Continued)

the choice of orography is crucial to the simulation of the Indian monsoon circulation and precipitation, with the mean orography yielding realistic results.

Two experiments were performed to investigate separately the effects of changing the vegetation type and the initial soil wetness over India on the simulated In-

dian monsoon. These experiments suggest that misrepresentations of these land surface characteristics are not primarily responsible for the poor Indian monsoon simulation of the control integration.

We have also performed a boreal summer experiment in which the solar radiation reaching the surface

of the Indian subcontinent is perturbed by eliminating the cloud radiative interaction over the region (including the longwave radiation interaction). While this perturbation does result in increased Indian monsoon rainfall, the enhancement is too small to correct the deficiencies noted in the control simulation.

The model formulation is outlined in section 2. The control simulation of the Indian summer monsoon is presented in section 3. The orography sensitivity experiments and a linear analysis of some of the results are discussed in section 4. The results from the sensitivity experiments involving vegetation, soil wetness, and cloudiness are discussed in section 5. A summary is given in section 6.

## 2. The model

The COLA GCM is based on a modified version of the National Meteorological Center (NMC) global spectral model used for medium-range weather forecasting [see Sela (1980) for original NMC formulation; see Kinter et al. (1988) for the modified version]. The land surface parameterization was changed to the SiB biophysical formulation after Sellers et al. (1986) by Sato et al. (1989) and later simplified by Xue et al. (1991). The model used in these experiments is the same as that presented by Xue et al. (1991) except that an interactive cloud radiation scheme was added (Hou 1990; after Slingo 1987) and a gravity-wave drag parameterization was included (Vernekar et al. 1992; after Alpert et al. 1988).

The COLA GCM is a global spectral model with rhomboidal truncation at zonal wavenumber 40. The model physical calculations are done on a  $1.8^\circ$  lat by  $2.8^\circ$  long grid. The vertical structure of the model is represented by 18 unevenly spaced levels using sigma (Phillips 1957) as the vertical coordinate. The spacing of the levels is such that greater resolution is obtained near the earth's surface and at the tropopause. In addition to the parameterizations mentioned above, the COLA GCM includes parameterizations of solar radiative heating (Lacis and Hansen 1974), terrestrial radiative heating (Harshvardhan et al. 1987), deep convection (Anthes 1977; after Kuo 1965), shallow convection (Tiedke 1984), large-scale condensation, and a turbulence closure scheme for subgrid-scale exchanges of heat, momentum, and moisture (Miyakoda and Sirutis 1977; Mellor and Yamada 1982).

## 3. Control integration

The COLA GCM described in section 2 was integrated for 90 days, starting from the National Meteorological Center (NMC) analysis of the observed atmospheric initial state at 0000 UTC on 2 June 1988. The GCM can change the temperature of sea ice, but does not create or destroy it; nor does it alter the surface temperature of open water (SST). Time-varying ob-

served SST (Reynolds 1988) was used from  $50^\circ\text{S}$  to  $60^\circ\text{N}$  and the COADS/ICE climatological SST (Reynolds 1988) was used elsewhere.

We have compared the global features of the June–July–August (JJA) 1988 time mean of the control integration to the corresponding time mean of the analyses of the observed data from NMC and the European Centre for Medium-Range Weather Forecasts (ECMWF). In general, the control integration reasonably represents the observed features in the wind, temperature, geopotential height, sea level pressure (SLP), and precipitation fields. A major weakness of the JJA simulation is in its representation of the Asiatic monsoon circulation and precipitation.

The control JJA precipitation field contains a good representation of the intertropical convergence zone (ITCZ) and South Pacific convergence zone (SPCZ) in the Pacific, as well as the ITCZ across South America and the Atlantic (not shown). The JJA 1988 observed precipitation is shown in Fig. 1a. This observed field is a combination of the Global Precipitation Climatology Center [of the Global Precipitation Climatology Project, Janowiak and Arkin (1991)] gridded station data over land, and precipitation derived from Microwave Sounding Unit satellite data over ocean (Spencer 1993). The observed precipitation is plotted on the original  $2.5^\circ$  by  $2.5^\circ$  grid, and the model precipitation, as well as all the remaining figures in this paper are plotted on a  $4^\circ$  latitude by  $5^\circ$  longitude grid. Thus, the model precipitation has been effectively “smoothed” somewhat. The GCM simulates the precipitation maximum of the African monsoon, but produces a very poor simulation of the Indian monsoon precipitation, missing the observed west coast maximum and placing the Bay of Bengal maximum too far northward (Fig. 1b). Much of peninsular India has extremely low simulated precipitation of  $4\text{ mm day}^{-1}$  or less. This lack of Indian monsoon rainfall has been noted in previous versions of the GCM (Fennessy and Shukla 1990), and is in contrast to the  $6\text{--}10\text{ mm day}^{-1}$  observed at stations over most of India.

The control JJA 850-mb vector wind field (Fig. 1d) is broadly similar to the JJA 88 ECMWF analysis (Fig. 1c). However, the simulated southwest monsoon flow penetrates much too far northward into India and the entire cross-equatorial circulation is weaker than observed. The southerly jet over southeast China, which is related to the southeast Asian monsoon (Lau et al. 1988), is simulated much stronger than that observed. The magnitude of the northeast and southwest trade winds over Africa is excessive, although their convergence at  $15^\circ\text{--}20^\circ\text{N}$  is fairly well simulated.

At 200 mb, the control correctly simulates the strong equatorial easterlies observed throughout the monsoon belt, as well as the maximum over the Arabian Sea and southern India (not shown). The south Asian anticyclone associated with the monsoon is also fairly well simulated, but its center is about  $5^\circ$  north of the ob-

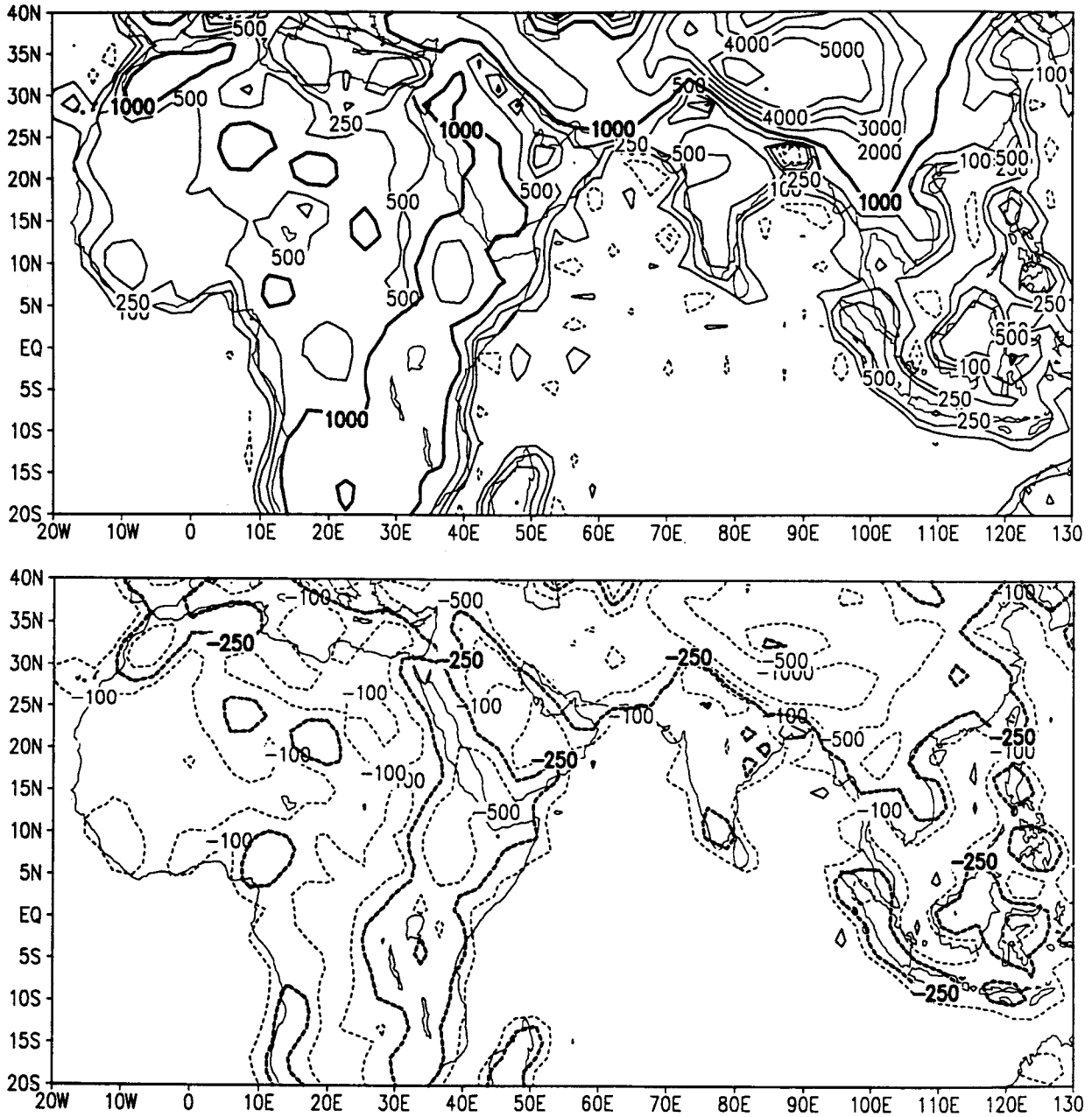


FIG. 2. Orography for GCM integrations (a) control and (b) mean orography minus control. Contours are  $\pm 100, 250, 500, 1000, 2000, 3000, 4000, 5000,$  and  $6000$  m. Dashed contours are negative.

served latitude ( $25^{\circ}\text{N}$ ). The westerlies at  $30^{\circ}$ – $40^{\circ}\text{N}$  are well placed, but much weaker than those observed.

The integrations performed for each of the sensitivity experiments presented in sections 4 and 5 were identical to the control integration except for the one physical parameter being tested. Specifically, they were all 90-day integrations initialized from the observed atmospheric state on 2 June 1988 performed with the same COLA GCM as used in the control integration.

#### 4. Orography experiments

##### a. GCM experiment

An experiment was performed to investigate the impact of the use of an enhanced silhouette orography in the COLA GCM. A “mean orography” was computed on the COLA GCM Gaussian grid from the U.S. Navy 10-min resolution modal terrain height data. The original silhouette orography used in the control integration

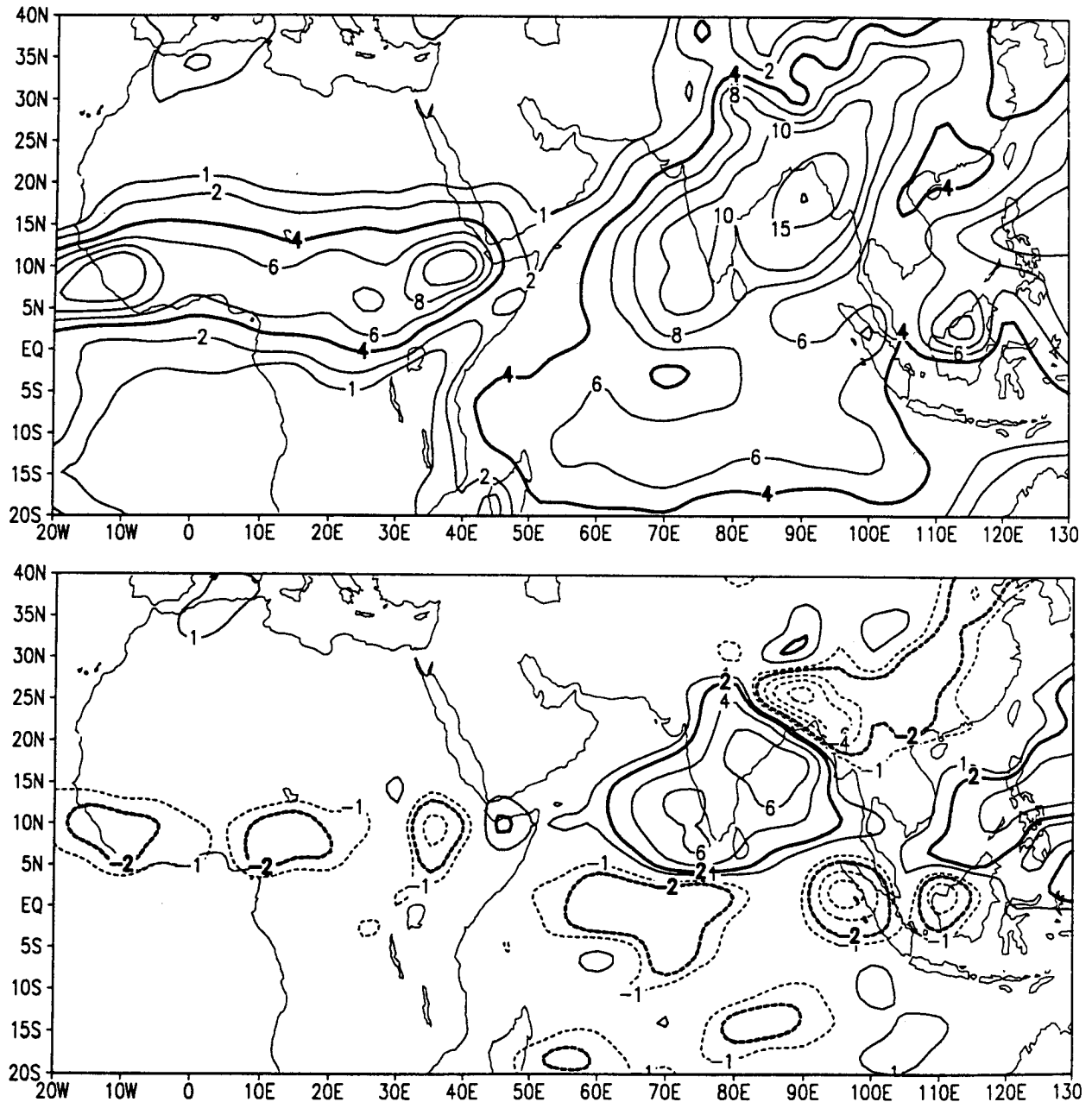


FIG. 3. JJA (a) mean orography integration precipitation. Contours are 1, 2, 4, 6, 8, 10, 15, 20, and 25 mm day<sup>-1</sup>. (b) Mean orography integration minus control precipitation difference. Contours are  $\pm 1$ , 2, 4, 6, and 8 mm day<sup>-1</sup>. Dashed contours are negative.

is shown in Fig. 2a, the mean orography minus silhouette orography difference is shown in Fig. 2b. These figures show only the Indian monsoon region, although the new orography was used globally. There are large differences between the mean and the silhouette orography. In the vicinity of the Himalayas (as well as the Andes, not shown) the mean orography maxima are more than 1 km lower than those of the silhouette orography.

The JJA mean precipitation from the mean orography integration and its difference from that in the control integration are shown in Figs. 3a and 3b, respectively. The rainfall over the entire Indian peninsula is increased by at least 3 mm day<sup>-1</sup> in the new integration. The mean rainfall of the new integration compares favorably with that observed (Fig. 1a), in contrast to that of the control integration (Fig. 1b). The simulation with mean orography also simulates the max-

ima off both coasts more realistically, although the maxima are still somewhat weak compared to observed.

At 850 mb the mean orography integration JJA southwest monsoon flow (not shown) is  $2\text{--}4\text{ m s}^{-1}$  stronger than that of the control (Fig. 1d) and is well positioned, albeit still weak compared to that observed (Fig. 1c). The low-level westerly flow across the Bay of Bengal is also accelerated in the mean orography experiment, becoming slightly stronger than that observed. At 200 mb, the mean orography intensifies the equatorial easterlies in the central and western Indian Ocean and the westerly jet north of India, both by  $5\text{--}10\text{ m s}^{-1}$ , in better agreement with the observed flow compared to the control integration (not shown).

### b. Linear model results

We performed additional experiments with a steady linear primitive equation model of perturbations about a zonally symmetric basic state to evaluate the changes in the time-mean atmospheric flow directly forced by the changes in the elevation of the lower boundary. As precipitation is known to be sensitively dependent on both the GCM's subgrid-scale parameterizations and the simulated low-level tropical circulation, we focus on the low-level atmospheric response. These simple experiments are designed to test whether the precipitation differences could result from a modulation of the orographically forced stationary circulation in the lower tropical troposphere. The underlying hypothesis is that precipitation in the tropics is forced by low-level moisture convergence, and that changes in the orographically forced waves modulate the low-level mass and moisture convergence. We hypothesize that boundary-layer mass and, hence, moisture convergence produced by orographically forced stationary waves, will enhance moist convection in tropical regions where the conditions for convection are favorable, and conversely that orographically forced divergence will suppress convection. Nigam (1992, personal communication) has shown that this effect is important in explaining lower-tropospheric monsoon circulation and rainfall anomalies over Indochina during 1987 and 1988.

We use a steady linear primitive equation model on the sphere having the same 18 sigma levels as in the GCM to calculate the stationary wave response to the two surface orographies. The steady linear spectral model, described in Schneider (1989, 1990), was truncated meridionally at wavenumber 15 and zonally at wavenumber 8, and the momentum dissipation in the planetary boundary layer was parameterized as in the GCM via vertical diffusion of horizontal momentum. The damping coefficient in the steady linear model was, however, prescribed to vary only in the vertical, and the drag coefficient was set equal to a constant. The values of vertical diffusion and drag coefficients were

those of Schneider (1989) scaled for the unequally spaced sigma levels of the current GCM. A correction was added to the horizontal del fourth diffusion to make it act along constant pressure surfaces, also as in this version of the GCM, and the same horizontal diffusion coefficient was used for temperature, vorticity, and divergence,  $10^{17}\text{ m}^4\text{ sec}^{-1}$ . The zonally symmetric basic state consisting of the zonal wind, the absolute temperature, and the zonal-mean profile of the logarithm of surface pressure, was calculated from the climatology of ECMWF summer (JJA) analyses extending from 1980 to 1988.

The mean orography minus silhouette orography JJA precipitation difference from the GCM is shown in Fig. 4a. Significant precipitation differences occur over both land and oceans, but are mainly confined to tropical latitudes. The corresponding difference between the two steady linear model solutions using the two different orographies is shown in Fig. 4b, which shows the 1000-mb eddy divergence difference. Negative values represent relative low-level convergence and therefore enhanced precipitation according to the simple hypothesis stated here. There is a clear correspondence between the precipitation difference (Fig. 4a) and the 1000-mb divergence anomaly calculated using the linear model, particularly over the Indian subcontinent and the Indian Ocean, Africa, Indonesia, and southeast China. Divergence anomalies and precipitation anomalies are unrelated in regions of very small precipitation (such as the eastern Pacific or the Sahara desert). There is no apparent relationship between the fields in the extratropics. The linear model produces significant low-level divergence anomalies in tropical South and Central America. We speculate that these may be associated with noticeable effects on precipitation during the rainy seasons in these locations. These experiments suggest that modulations of the orographically forced stationary waves in the tropical and subtropical lower troposphere can potentially have a strong influence on the distribution of precipitation in these regions through modulations of the low-level moisture convergence field. The low-level convergence in the linear model results from the kinematic effect of air blowing over the mountains at the lower boundary (specified as a boundary condition) and the dynamical response of the atmosphere to this forcing, which affects convergence both near the mountains and in remote regions. A separate calculation of the kinematic effect reveals that the dynamical response is as important as the kinematic effect in our results (not shown).

The linear model low-level convergence anomaly has maximum amplitude near the ground and decays rapidly with height (not shown). These results should be viewed with some caution over land, since some of the structure could be an artifact of vertical extrapolation below the surface. The magnitude of the linear model low-level convergence anomaly is about

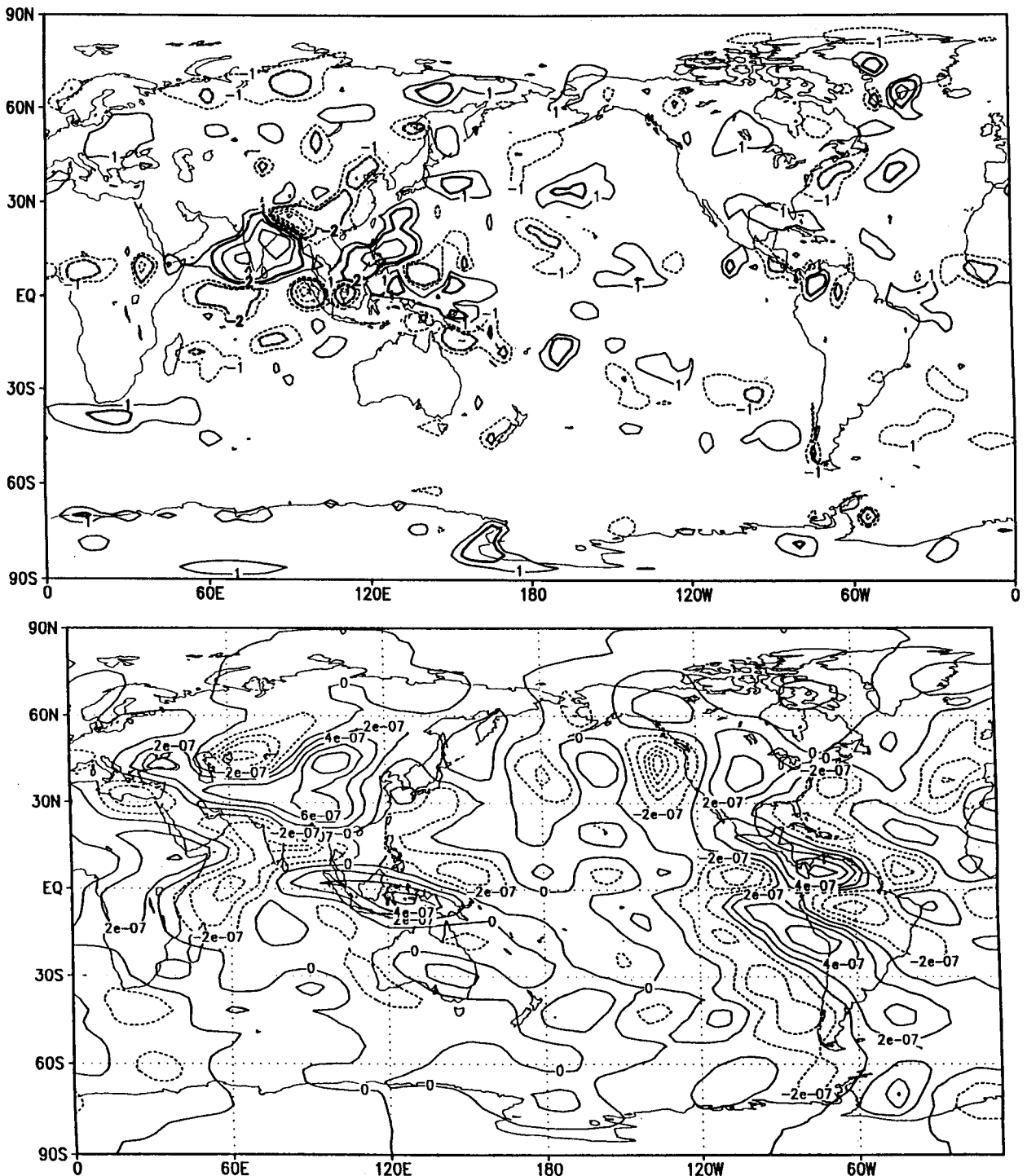


FIG. 4. (a) Mean orography minus silhouette orography GCM precipitation difference for JJA mean. Contours are 1, 2, 4, and 8 mm day<sup>-1</sup>. (b) Eddy divergence difference at 1000 mb between linear model solution forced by silhouette and mean orographies. Contour interval is  $2 \times 10^{-7}$  sec<sup>-1</sup>. Dashed contours are negative.

a factor of 4 smaller than that found in the GCM. This is consistent with our expectation of a positive feedback between deep convection and boundary-

layer moisture convergence in the GCM, which is absent from the linear model because thermal forcing is not included.



### 5. Vegetation, soil wetness, and cloudiness experiments

To check the sensitivity of the Indian monsoon to local vegetation, we replaced the mix of winter wheat and broadleaf deciduous trees over India with all broadleaf deciduous trees. This results in significant increases in the vegetation cover, leaf area index, surface roughness, and soil depths. However, the JJA mean precipitation in this integration was within  $0.5 \text{ mm day}^{-1}$  of that in the control integration throughout India (not shown). There was only a slight change in evaporation, and the most coherent change between the two simulations was a  $1^\circ\text{C}$  reduction in the JJA mean surface temperature across India.

A separate experiment was designed to determine the sensitivity of the Indian monsoon simulation to changes in the soil wetness field used to initialize the control integration. The control integration is initialized with a soil wetness field derived from the Mintz and Serafini (1984) climatological soil moisture field and is very dry over all of India, with values ranging from 17% to 33%. A wet soil integration was performed in which the initial state soil wetness over the entire model grid was set to the maximum allowed by SiB for the given vegetation type of each grid box, generally 70%–80%. The resulting initial soil wetness anomaly is very large over India, with values ranging from 30% to over 50% wetter than in the control integration. As in the otherwise identical control integration, the GCM predicts the evolution of the three soil wetness layers throughout the 90 days of integration. The JJA mean of the wet soil minus control precipitation difference (Fig. 5a) shows that the precipitation was increased by  $1\text{--}2 \text{ mm day}^{-1}$  over central and southern India in the wet soil integration. This clearly is an improvement over the very dry control simulation in this region. However, the JJA mean precipitation of the wet soil integration has a relative minimum over peninsular India, as in the control experiment.

An experiment was conducted to test the simulated Indian monsoon sensitivity to cloud–radiation interaction. The clouds were artificially suppressed in the radiative calculation over the entire Indian subcontinent for the whole season. The change in JJA mean precipitation is shown in Fig. 5b. A  $2 \text{ mm day}^{-1}$  increase in precipitation was produced over north central India. An increase of similar magnitude was produced over eastern China, and a decrease in precipitation of about the same amount was found over the Bay of Bengal and the Indian Ocean south of the peninsula. Although the increase in precipitation over India was an improvement in the monsoon simulation, it was too small by about one half and not well correlated with the control integration error.

### 6. Discussion

This study was motivated by the very weak simulation of Indian monsoon precipitation in boreal sum-

mer integrations with the COLA GCM. This deficiency was noted in several versions of the GCM, and appeared to be independent of the choice of initial and SST boundary conditions used in the seasonal integrations.

The orography experiment revealed that the use of enhanced silhouette orography resulted in the poor simulation of Indian monsoon rainfall in the control version of the COLA GCM. The use of mean orography resulted in a better simulation of both the magnitude and pattern of the seasonal mean Indian monsoon precipitation, as well as an improved simulation of both the upper- and lower-level flow. Experiments performed with a steady linear primitive equation model on the sphere suggest that the improved Indian monsoon precipitation simulation obtained through the use of the mean orography is primarily due to modulations of the orographically forced stationary waves in the lower troposphere. An examination of the atmospheric heating profile above the Asian landmass reveals no major differences between the simulations done with the silhouette orography and the mean orography. Thus, it appears that the hypothesis supported by the linear model is a plausible explanation for the improvement in the Indian monsoon simulation.

Enhancing the vegetation over India had little effect on the simulation of the Indian monsoon. The local evapotranspiration was only slightly changed from the low values simulated in the control integration. This lack of impact is likely related to the low mean evapotranspiration over India in both the control and sensitivity integrations, which is due to the very dry soil conditions over premonsoon India. This dryness persists in both integrations due to the very low simulated precipitation.

A greater impact was obtained in a soil wetness sensitivity experiment in which the global soil wetness was set to saturated values. The soil wetness over India was changed from extremely dry values in the control integration to extremely wet values in the sensitivity experiment. This resulted in an enhancement of the Indian monsoon precipitation by about  $2 \text{ mm day}^{-1}$ , which only partially corrected the model deficiency. However, this impact suggests the possible importance of soil wetness in tropical precipitation simulations.

A cloudiness sensitivity experiment was conducted in which the radiatively active clouds over India were removed throughout the seasonal integration. This resulted in a  $2 \text{ mm day}^{-1}$  increase in the Indian monsoon precipitation, again too little to correct the basic model deficiency.

Additional integrations with the COLA GCM using the mean orography have successfully simulated the Indian monsoon precipitation interannual variability between 1987 and 1988 (Fennessy and Shukla 1992), reaffirming that to correctly simulate an atmospheric anomaly, one must first correctly simulate the mean circulation. Finally, we should reiterate that all the bo-

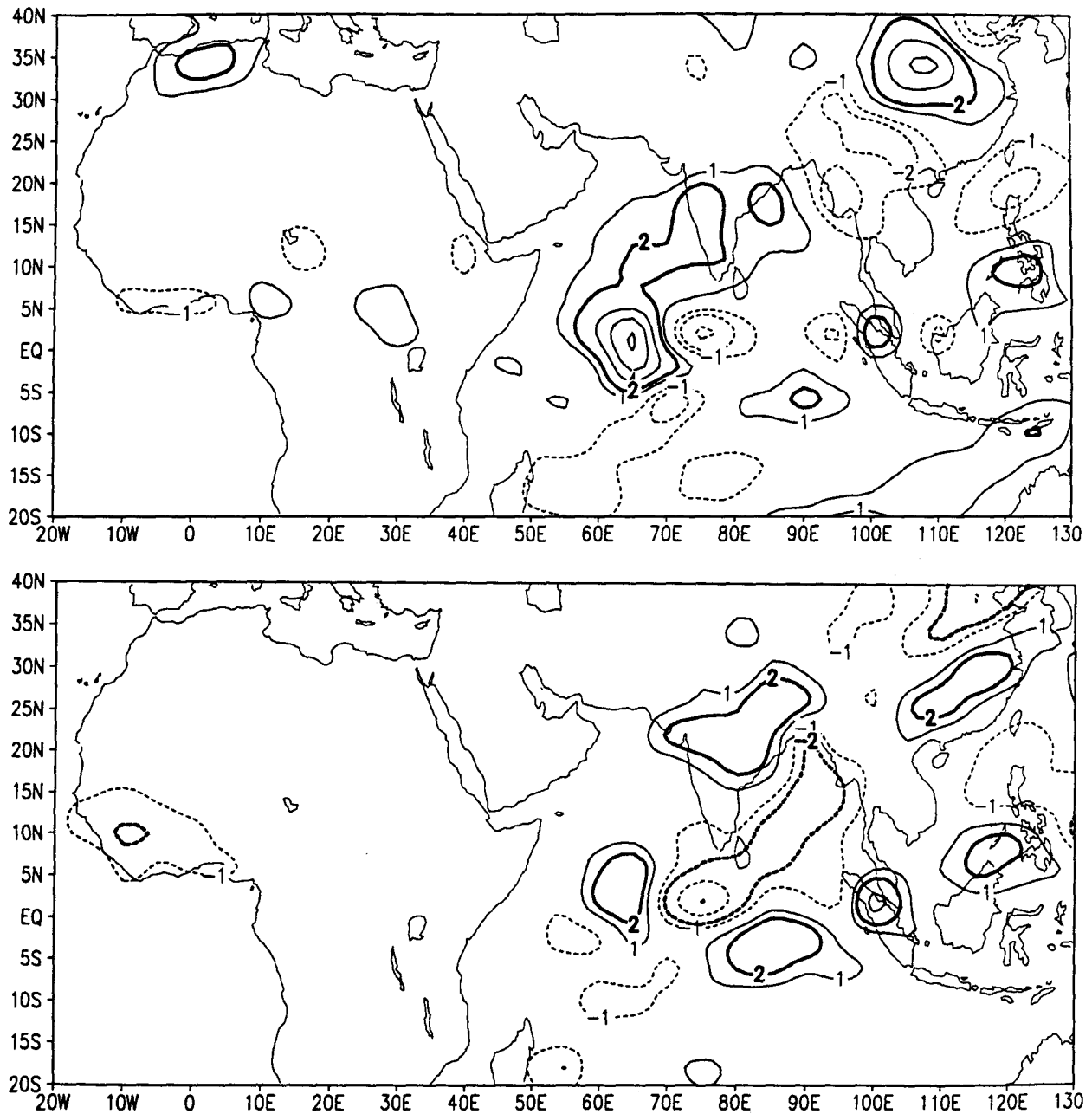


FIG. 5. JJA mean precipitation difference for (a) wet soil integration minus control and (b) no cloud integration minus control. Contours are  $\pm 1, 2, 4, 6,$  and  $8 \text{ mm day}^{-1}$ . Dashed contours are negative.

real summer seasonal integrations described here were initialized from observed atmospheric states for early June. The possible dependence of the simulation of the seasonal mean Indian monsoon on integration length is currently being investigated.

*Acknowledgments.* This research was supported by NASA Grants NAGW-558 and NAGW-2661, and by NSF Grant ATM-90-19296. The authors would like to thank Mr. John Janowiak for his help in obtaining

the GPCP gridded station precipitation data and Dr. Roy Spencer for providing the MSU oceanic precipitation product.

#### REFERENCES

- Alpert, J. C., M. Kanamitsu, P. M. Caplan, J. G. Sela, G. H. White, and E. Kalnay, 1988: Mountain induced gravity wave drag parameterization in the NMC medium-range forecast model. *Proc. Eighth Conf. on Numerical Weather Prediction*. Baltimore, Amer. Meteor. Soc., 726–733.

- Anthes, R. A., 1977: A cumulus parameterization scheme utilizing a one-dimensional cloud model. *Mon. Wea. Rev.*, **105**, 270–300.
- Barnett, T. P., L. Dümenil, U. Schlese, E. Roeckner, and M. Latif, 1989: The effect of Eurasian snow cover on regional and global climate variations. *J. Atmos. Sci.*, **46**, 661–685.
- Bhaskar Rao, D. V., K. Yamazaki, and A. Kitoh, 1991: Some GCM experiments of the Asian summer monsoon related to land boundary conditions. *Pap. Meteor. Geophys.*, **42**, 127–143.
- Druryan, L. M., 1981: The use of global general circulation models in the study of the Asian monsoon. *J. Climatol.*, **1**, 77–92.
- , 1982: Studies of the Indian summer monsoon with a coarse-mesh general circulation model. Part 1. *J. Climatol.*, **2**, 127–139.
- Fennessy, M. J., and J. Shukla, 1990: Influence of global SST on GCM simulations of the Northern Hemisphere monsoon circulations of 1987 and 1988. Report of the Second Session of the TOGA Monsoon Numerical Experimentation Group, WMO/TD-No. 392, WCP, WMO, Geneva, Appendix B, 1–20.
- , and —, 1992: Influence of global SST on GCM simulations of the Northern Hemisphere monsoon circulations of 1987 and 1988. Report of the MONEG workshop on Simulation of interannual and intraseasonal monsoon variability. WMO/TD-No. 470, WCP, WMO, Geneva, 2.37–2.45.
- Hahn, D. G., and S. Manabe, 1975: The role of mountains in the south Asian monsoon circulation. *J. Atmos. Sci.*, **32**, 1515–1541.
- Harshvardhan, R. Davies, D. A. Randall, and T. G. Corsetti, 1987: A fast radiation parameterization for general circulation models. *J. Geophys. Res.*, **92**, 1009–1016.
- Hou, Y.-T., 1990: Cloud–radiation–dynamics interaction. Ph.D. thesis, University of Maryland, 209 pp. [Available from University of Maryland, Dept. of Meteorology, College Park, MD 20742.]
- Janowiak, J. E., and P. A. Arkin, 1991: Rainfall variations in the tropics during 1986–1989, as estimated from observations of cloud-top temperature. *J. Geophys. Res.*, **96**, 3359–3373.
- Kinter, J. L., III, J. Shukla, L. Marx, and E. K. Schneider, 1988: A simulation of the winter and summer circulations with the NMC global spectral model. *J. Atmos. Sci.*, **45**, 2486–2522.
- Krishnamurti, T. N., and Y. Ramanathan, 1982: Sensitivity of monsoon onset to differential heating. *J. Atmos. Sci.*, **39**, 1290–1306.
- Kuo, H. L., 1965: On formation and intensification of tropical cyclones through latent heat release by cumulus convection. *J. Atmos. Sci.*, **22**, 40–63.
- Lacis, A. A., and J. E. Hansen, 1974: A parameterization for the absorption of solar radiation in the earth's atmosphere. *J. Atmos. Sci.*, **32**, 118–133.
- Lau, K. M., G. J. Yang, and S. H. Shen, 1988: Seasonal and intra-seasonal climatology of summer monsoon rainfall over East Asia. *Mon. Wea. Rev.*, **116**, 18–37.
- Luo, H., and M. Yanai, 1984: The large-scale circulation and heat sources over the Tibetan Plateau and surrounding areas during the early summer of 1979. Part II: Heat and moisture budgets. *Mon. Wea. Rev.*, **112**, 966–989.
- Mellor, G. L., and T. Yamada, 1982: Development of a turbulence closure model for geophysical fluid problems. *Rev. Geophys. Space Phys.*, **20**, 851–875.
- Mesinger, F., Z. I. Janjic, S. Nickovic, D. Garilov, and D. G. Deaven, 1988: The step mountain coordinate: Model description and performance for cases of Alpine lee cyclogenesis and for a case of Appalachian redevelopment. *Mon. Wea. Rev.*, **116**, 1493–1518.
- Mintz, Y., and Y. V. Serafini, 1984: Global fields of monthly normal soil moisture as derived from observed precipitation and estimated potential evapotranspiration. Land surface influences on weather and climate. Final Tech. Report, NASA-CR-173575, 182 pp.
- Miyakoda, K., and J. Sirutis, 1977: Comparative integrations of global spectral models with various parameterized processes of subgrid scale vertical transports. *Beitr. Phys. Atmos.*, **50**, 445–447.
- Philips, N. A., 1957: A coordinate system having some special advantages for numerical forecasting. *J. Meteor.*, **14**, 184–185.
- Reynolds, R. W., 1988: A real-time global sea surface temperature analysis. *J. Climate*, **1**, 75–86.
- Sato, N., P. J. Sellers, D. A. Randall, E. K. Schneider, J. Shukla, J. L. Kinter III, Y.-T. Hou, and E. Albertazzi, 1989: Effects of implementing the Simple Biosphere Model in a general circulation model. *J. Atmos. Sci.*, **46**, 2757–2782.
- Schneider, E. K., 1989: A method for solution of a steady linearized general circulation mode. *Mon. Wea. Rev.*, **117**, 2137–2141.
- , 1990: Linear diagnosis of stationary waves in a general circulation model. *J. Atmos. Sci.*, **47**, 2925–2952.
- Sela, J. G., 1980: Spectral modeling at the National Meteorological Center. *Mon. Wea. Rev.*, **108**, 1279–1292.
- Sellers, P. J., Y. Mintz, Y. C. Sud, and A. Dalcher, 1986: A Simple Biosphere Model (SiB) for use within general circulation models. *J. Atmos. Sci.*, **43**, 505–531.
- Slingo, J. M., 1987: The development and verification of a cloud prediction scheme for the ECMWF model. *Quart. J. Roy. Meteor. Soc.*, **103**, 29–43.
- Spencer, R., 1993: Global oceanic precipitation from the MSU during 1979–91, and comparisons to other climatologies. *J. Climate*, **6**, 1301–1326.
- Tiedtke, M., 1984: The effect of penetrative cumulus convection on the large-scale flow in a general circulation model. *Beitr. Phys. Atmos.*, **57**, 216–239.
- Vernekar, A., B. Kirtman, J. Zhou, and D. Dewitt, 1992: Orographic gravity-wave drag effects on medium-range forecasts with a general circulation model. *Physical Processes in Atmospheric Models*, D. R. Sikka and S. S. Singh, Eds., Wiley Eastern Limited, 295–307.
- Wallace, J. M., S. Tibaldi, and A. J. Simmons, 1983: Reduction of systematic forecast errors in the ECMWF model through the introduction of an envelope orography. *Quart. J. Roy. Meteor. Soc.*, **109**, 683–717.
- WMO, 1990: Report of the Second Session of the TOGA Monsoon Numerical Experimentation Group. WMO/TD-No. 392, WCP, WMO, Geneva, 56 pp.
- Xue, Y., P. J. Sellers, L. Kinter, and J. Shukla, 1991: A simplified biosphere model for global climate studies. *J. Climate*, **4**, 345–364.